Journal of Engineering Sciences
Assiut University
Faculty of Engineering
Vol. 45
No. 3
May 2017
PP. 301 – 323

ENERGY ABSORPTION AND DAMAGE OF INELASTIC SDOF STRUCTURES UNDER BLAST LOADS

Abbas Moustafa [1], Basma. M. F. Hassan [2, *]

[1] *Associate Professor, Department of Civil Engineering, Minia University, Minia, Egypt*
[2] *Civil engineer, Directors Housing and Utilities, Aswan, Egypt*

Received 29 March 2017; Accepted 29 April 2017

ABSTRACT

Important and critical structures should be designed to resist transient extreme loads such as high velocity impacts and explosions. Blast-resistant design of structures includes architectural design and structural design against explosion forces. Blast loads could be internal due to explosion of gas pipes or external due to chemical bombs and car attacks. During the last few years, Egypt witnessed terrorist bombs and car attacks on important structures. These events caused large life losses and led to severe damage and collapse of several heritage and security buildings. In this paper, the response and damage of single-degree-of-freedom (SDOF) structures to blast loads are presented. The blast load is modeled as a time-variant function with positive and negative pressure zones. Firstly, the governing nonlinear differential equation of motion for SDOF of inelastic structures under blast load is provided. Subsequently, the solution of this equation is obtained using numerical integration of the equation of motion in the MATLAB platform [1]. Finally, the definition of various energy terms dissipated by the structure and associated damage indices are given. The formulation developed is numerically demonstrated with reference to energy dissipated and damage of a simple structure modeled as a SDOF inelastic system to blast load. A new scalar index based on damage indices is proposed. These measures are of essential importance since they provide quantitative measures on damage level of the structure and necessary repair.

Keywords: blast load, damage index, explosion, hysteretic energy, inelastic structures, plastic behavior.

1. Introduction

The major use of explosives has been in warfare such as bombs, explosive shells, torpedoes and missile warheads. On the other hand, the peaceful use of explosives is to break rocks in mining. Also, explosions are used in malting roads and tunnels inside mountains and in extracting important materials such as gold and phosphate. Explosions are used also in demolishing of structures that are deteriorated or damaged due to aging etc. or which were constructed illegally. Unlike earthquakes, floods and cyclones which represent natural disasters, blast loads represent a man-made disaster caused by humans. Note that, there are two types of loads static loads (live loads and dead loads) and dynamic loads (earthquake

* Corresponding author.
Email address: *eng_basmafathy201012@yahoo.com*

loads, snow loads, impact loads, water waves, Air plan, machine vibration, *etc*…..). Previous researches consider blast loads are dynamic loads [2]. Explosions produce sudden shocks with extreme transient loads in a very short time duration.

An explosion is a release of energy with chemical reactions on a large scale in a short period of time (usually a fracture of a second). Explosions can be categorized on the basis of their nature as nuclear, physical and chemical events. The detonation of a condensed high explosive generates hot gases under a high pressure of up to 30 MPa, a temperature of about 3000 - 4000 C° and shock waves which propagate a high-pressure gas travelling with very high velocity about 7000 m/s to areas far from the origin of the incident [3, 4 and 5]. The hot gas expands forcing out the volume it occupies. As a consequence, a layer of compressed air resulting in a blast wave is generated in front of this gas volume containing most of the energy released by the explosion.

Blast wave instantaneously increases to a value of pressure above the ambient atmospheric pressure and propagates in all directions (figure 1). This is referred to as the side-on overpressure that decays as the shock wave expanding outward from the explosion source. After a short time period, the pressure behind the front may suddenly drop below the ambient pressure. During such a negative pressure phase, a partial vacuum is created and air is sucked in. This is also accompanied by high suction winds that carry the debris for long distances away from the explosion source [4].

The observed characteristics of air blast waves are found to be affected by the physical properties of the explosion source. Figure 1 shows a typical blast pressure profile. At the arrival time t_{A}, following the explosion, pressure at that position suddenly increases to a peak value of overpressure, P_{s} over the ambient pressure, P_0. The pressure then decays to ambient level at time t_d, then decays further to an under pressure P_{s^-} (creating a partial vacuum) before eventually returning to ambient conditions at time $t_{\mathrm{d}^+} + t_{\mathrm{d}^-}$. The negative phase is of a longer duration and a lower magnitude than the positive duration. It is often neglected for design. This approach is generally conservative because component response calculated without consideration of the negative phase can be significantly greater than measured component response in blast tests [6]. As the stand-off distance increases, the duration of the positive-phase blast wave increases resulting in a lower-amplitude, longer-duration shock pulse [3]. The quantity P_{s} is usually referred to as the peak side-on overpressure, incident peak over-pressure or merely peak overpressure [5]. The blast load total duration ranges from 0.001 to about 0.10 s [7].

Subsequently, the investigation of effects of explosion loads on engineering structures has begun for 70 years [7]. Following are examples of international codes and scientific research that gave us a comprehensive view of defining and modeling of blast loads and their effects on structures and buildings. In 1959, department of the Army released a technical manual entitled "structures to resist the effects of accidental explosions". The revised edition of this manual, known as U. S. TM 5-1300 [5] is used by civilian organizations and military for designing structures to, (1) prevent the propagation of explosion, (2) provide protection for personal and (3) provide guidance to designers on the blast design of structural components and connections subjected to blast loads. Indian Standard code [8] covers the criteria for design of structures for blast effects of explosions above ground. Whereas, the U.S. Army manual [9] gives a useful screening tool for assessing blast loads when it considers explosive device and location. Whereas, the American Society of Civil Engineers document [10] focuses on blast design of components

subjected to industrial explosions. Eurocode [11] gives rules and strategies for protecting buildings against accidental actions. The U.S. Army corps of engineers [12] distributes SDOF blast effects design spreadsheets for the design and analysis of structural components subject to blast loads. Canadian Standard Association [13] considers the design and assessment of buildings subjected to blast loads and achieving suitable levels of building safety.

Over the past five decades, researches have been undertaken in the modeling of blast pressure on buildings and structures [2, 14, 15, 16 and 17]. Previous research provides an accurate description of explosion and characteristics of the blast wave by developing mathematical representations for important explosions [9, 14, 18, 19, 20, 21, 22, 23 and 24].

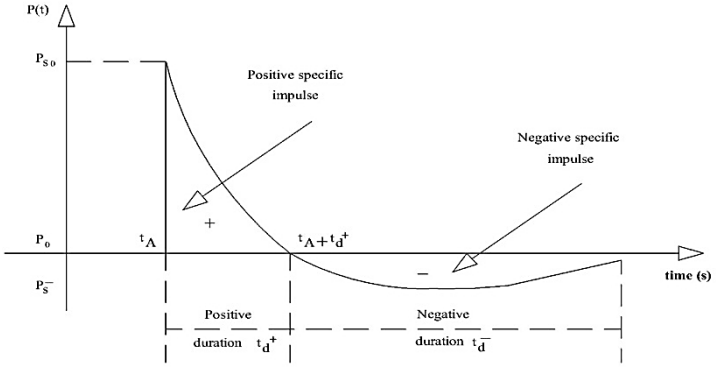

Fig. 1. Blast wave-pressure time-history [5].

Fertice [25] has studied the computation of blast loading on aboveground structures. LZA & Gilsanz and LZA *et al*. [26 and 27] have reviewed a large number of data in this field from the Second World War. Tens of thousands of records of bomb damage have been compiled referring to England, France, Germany and Japan. Simplified elastic perfectly plastic resistance functions for concrete elements may ignore the accurate nonlinear behavior of concrete other tri-linear and fiber models may provide accurate modeling for concrete structures under blast loads. Vrom [28 and 29] describes the idealized blast loads, the blast-structure interaction, and the response of SDOF systems to blast loading, the dynamic load factor, pressure impulse diagrams and the modeling of a structure as a SDOF system under blast load.

Marchand [30] reviewed the contents of American Institute of Steel Construction (AISC). He also studied the dynamic response of steel structures to blast loads focusing on the behavior of columns and connections. Ngo *et al*. [4] gave an overview on the analysis and design of structures subjected to blast loads. The study focuses on the design considerations against extreme events such as a bomb blast. Structures, which are designed for resisting explosion and impact, are permitted to contribute all of their resistance, to absorb damage locally and to insure the integrity of the entire structure. It is likely that local failure may happen, due to the uncertainty associated with the loads.

If a building is designed for a blast, the concrete components usually perform better compared to other materials such as timber and other metals such as aluminum and steel. This could be attributed to more mass, more damping and energy absorbing capacity of concrete [31]. Indeed, the analysis and design of structures subjected to blast loads require a detailed understanding of the blast phenomenon and the dynamic response of various structural elements.

2. Measures of explosive charge using TNT equivalent

Explosives are different according to their explosion characteristics such as effectiveness, detonation rate and amount of energy released. So, it is necessary to have a datum to assess the detonation characteristics of each type of explosive material. Therefore, the use of TNT as the reference explosive is universal [32].

The first stage in quantifying blast waves is to change the actual mass of the charge into a TNT equivalent mass. For achieving this we should multiply the mass of explosive by a conversion factor based on its specific energy and that of TNT. Table 1 shows the conversion factors for a number of explosives [32]. An alternative approach which is described in U. S. TM5-855-1 [9] makes use of two conversion factors. Choosing any one of these factors depends on peak overpressure or impulse. Thus, for compound B the equivalent pressure factor is 1.11 while that for impulse is 0.98 (see Table 1).

Table 1.
Conversion factors for explosives [32].

Explosive	Mass specific Energy Q_x(kj/kg)	TNT Equivalent Q_x/Q_{TNT}
Compound B (60%RDX,40%TNT)	5190	1.148
RDX (Cyclonite)	5360	1.185
HMX	5680	1.256
Nitroglycerin (liquid)	6700	1.481
TNT	4520	1.000
Blasting Gelatin*	4520	1.000
Nitroglycerin dynamite 60%	2710	0.600
Semtex	5660	1.250

Note: * 91.0 % nitroglycerin, 7.9 % nitrocellulose, 0.9 % antacid, 0.2 % water.

3. Basic parameters of the explosion

A blast load can be defined for blast design purposes in terms of several parameters. These parameters are overpressures, impulse and scaled distance, which represent the combined effects of charge weight and standoff distance. Other parameters include the explosion wave front velocity U_s and the maximum dynamic pressure q_s.

Namely, the explosion wave front velocity U_s and the maximum dynamic pressure q_s are given as [2, 19 and 22]:

$$U_s = a_0\sqrt{\frac{6p_s+7p_0}{7p_0}} \tag{1}$$

$$q_s = \frac{5{p_s}^2}{2(p_s+7p_0)} \tag{2}$$

where a_0 is the speed of sound in air at ambient pressure (355 m/s), p_s is the peak static overpressure at the wave front in bar and p_0 is the atmospheric pressure of about 1 bar or 101 kpa.

Mathematical relations for the maximum (peak) static overpressure (p_s) have been presented in the literature [4, 14, 23 and 24]. Therefore, p_s has typically been correlated with the scaled distance parameter (z) which is defined by Mays and Smith [21] as follows:

$$z = \frac{R}{w^{\frac{1}{3}}} \tag{3}$$

Where R is the stand-off distance in meters and *w* is the charge weight of the blast in kg based on TNT equivalence. For example, in 1993, the blast occurred at the World Trade Centre (WTC) has a charge weight of 816.5 kg TNT [20] and the bomb of April 1995 of the Alfred P. Murrah Federal Building in Oklahoma City has a charge weight 1800 kg of high explosives and located 5 m from the north face of the building and about 12–15 m from the east end [31]. Dharaneepathy *et al*. [33] studied the effect of the stand-off distance on tall shells of different heights.

Brode [14] introduced a mathematical relationship to calculate the peak overpressure in bars as follows [4]:

$$p_s = \frac{0.975}{z} + \frac{1.455}{z^2} + \frac{5.85}{z^3} - 0.019; \quad (0.1 \text{ bar} < p_s < 10 \text{ bar}) \tag{4-a}$$

$$p_s = \frac{6.7}{z^3} + 1; \qquad (p_s > 10 \text{ bar}) \tag{4-b}$$

Newmark and Hansen [24] introduced a relationship to calculate the maximum blast overpressure p_s in bar, for a high explosive charge detonates at the ground surface as [4]:

$$p_s = 6784\left(\frac{w}{R^3}\right) + 93\left(\frac{w}{R^3}\right)^{\frac{1}{2}} \tag{5-a}$$

$$= \frac{6784}{z^3} + \frac{93}{z^{\frac{2}{3}}} \tag{5-b}$$

Mills [23] introduced another expression of the peak overpressure in kPa as [4]:

$$p_s = \frac{1772}{z^3} - \frac{114}{z^2} + \frac{108}{z} \tag{6}$$

Friedlander wave equation defines the rise and fall of the static over pressure $p_s(t)$ with time. Mathematically, this can be defined as [22] and [34]:

$$p_s(t) = 1.8\, p_s \left(1 - \frac{t}{Ts}\right) e^{\frac{-bt}{T_s}} \tag{7}$$

Herein, e is the exponential function, p_s is the peak overpressure, t is the time elapsed and the constant 1.8 accounts for the hemispherical blast effects (i.e. the reflection factor). The constant b is the parameter controlling the rate of wave amplitude decay. This parameter can be related to the ratio ($p_{s_{min}}/p_{s_{max}}$) as:

$$\ln\left(b\left|\frac{p_{s_{min}}}{p_{s_{max}}}\right|\right) + b + 1 = 0 \tag{8}$$

Alternatively, the stand-off distance can be given as [22]:

$$b = z^2 - 3.7z + 4.2 \tag{9}$$

and T_s is the duration of the positive blast pulse. T_s has been correlated with the stand of distance (R) by Smith [17]. This correlation can be mathematically approximated with a linear relationship between T_s and R in a log-log format with z being held constant, as follows:

$$\log_{10}\left(\frac{T_s}{W^{\frac{1}{3}}}\right) = -2.75 + 0.27 \log_{10}\left(\frac{R}{W^{\frac{1}{3}}}\right) \tag{10}$$

When blast waves encounter a solid surface or an object made of a medium denser than air, they will reflect it causing what is known as a reflected pressure p_r. Rankine and Biggs derived a mathematical expression that relates reflected pressure p_r and the specific heat ratio γ as follows [2] and [35]:

$$p_r = 2p_s + (\gamma + 1)q_s \tag{11}$$

Herein the air behaves as a real gas with a specific heat ratio $\gamma = \frac{C_p}{C_v}$. For air, γ is set equal to 1.4 [22]. Substituting q_s into this equation leads to:

$$p_r = 2p_s \left(\frac{7p_0 + 4p_s}{7p_0 + p_s}\right) \tag{12}$$

Reflected overpressure can be idealized by an equivalent triangular pulse of maximum peak pressure p_s and time duration t_d, which yields the reflected impulse i_r (e.g. [4, 5 and 21]):

$$i_r = \frac{1}{2} p_r t_d \tag{13}$$

Other blast wave parameter includes t_d which is the duration of the positive phase when the pressure is in excess of ambient pressure and ${i_s}^+$ the specific impulse of the wave which is the area under the pressure time curve from the moment of arrival, t_A, to the end of the positive phase and is given by:

$${i_s}^+ = \int_{t_A}^{t_A + t_d} p_s(t)dt \tag{14-a}$$

For the above Friedlander equation (7), the positive impulse can be analytically calculated as:

$${i_s}^+ = \frac{p_s T s}{b^2}[b - 1 + e^{-b}] \tag{14-b}$$

Brode [14] proposed the maximum value of negative pressure in the negative phase of the blast, given by:

$$p^- = -\frac{0.35}{z}; \;\; 1.6 < z \leq 2 \tag{15}$$

Note that, the negative phase of the overpressure is not important and can be ignored [6]. The associated specific negative impulse in this phase ${i_s}^-$ is given in terms of the positive impulse and the stand-off distance as follows:

$${i_s}^- \approx {i_s}^+ \left(1 - \frac{1}{2z}\right) \tag{16}$$

The next section shows the difference between explosions and earthquakes**.**

4. The difference between explosions and earthquakes

Explosion differs from earthquake ground motion in the amount of energy released for a very short duration of time. Earthquake duration usually ranges from (10-100 s) while blast duration ranges from (0.001-0.1 s) [36]. Accordingly, the total duration of an average duration earthquake is about 1000 times that of a blast load. Example for that, the time of the long ground shaking from the Northridge event is 12 s and the time duration of the Murrah Building blast is 9 ms [3]. On the other hand (Ngo *et al.*) [4], the average strain rate of a blast load is about 10^5 times that for average earthquakes as will be mentioned hereafter, see (figure 2). It is well known that strain rate is the change in strain of a material with respect to time ($\frac{d\varepsilon}{dt}$).

The nuclear bomb of a Hiroshima in 6 August 1945 created a blast equivalent to about 16 $\times 10^3$ t of TNT and contained about 64 kg (141 lb) of uranium-235 [37]. This blast is equivalent to an earthquake of magnitude 6 on the Richter's scale [36]. Similarly, Nagasaki bomb in 9 August 1945 is equivalent to 21 $\times$ 10^3 t of TNT. This event is equivalent to an earthquake of magnitude 6.1 on the Richter's scale [36].

As mentioned above, blast loads occur over a significantly shorter period of time than seismic loads. Thus, material strain rate effects become critical and must be accounted for in predicting connection performance for short duration loadings such as blast. Also, blast loads are generally applied non-uniformly to a structure, leading to a variation of load amplitude across the face of the building. This intern reduces blast loads on the sides and rear of the building away from the blast. Figure 2 shows the approximate ranges of the expected strain rates for different loading conditions. It can be seen that earthquake strain rate is located in the range of 10^{-3} to 10^{-1} s^{-1}, while blast pressures normally yield loads associated with strain rates in the range: 10^2 to 10^4 s^{-1} [4].

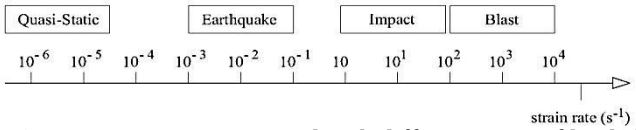

Fig. 2. Strain rates associated with different types of loads [4].

Blast loads are generally local loads, leading to local damage to the structure. Conversely, seismic loads are ground motions applied uniformly across the base or the foundation of the structure. Hence, all components in the structure are subjected to the shaking associated with this motion [3]. Note that a blast charge of about 12.5 $\times$ 10^3 t of TNT is equivalent to an earthquake of 5.0 Richter's magnitude that is capable of creating damage to the structure. The next section provides a brief review on structural response due to blast loading.

5. Structural response to blast loading

The simplest discretization of transient problems is by means of the SDOF approach [38, 39 and 40]. When a structure is subjected to sudden extreme transient loads such as plane attacks or blast loads, it experiences a rapid loading environment that results in sudden changes in stresses and strains in structural members during a short period of time compared to static loads such as live loads and dead loads [4]. Bangash [31], U. S. TM 5-1300 [41] and Ngo [5] provide the response analysis of building structures to explosions. The structural response depends on a number of factors including the structure layout in the plan, the structural detailing, the natural frequency, damping characteristics, material properties, explosive charge source and its range and DOFs as well as the individual components of the structure.

In this paper numerical integration of the differential equation governing the structural response of SDOF to blast loads is employed. These numerical methods are based on the mathematical equations that describe the basic laws of physics governing the structural response to the blast phenomenon. These principles include conservation of mass and energy. In addition, the physical behavior of materials is described by constitutive laws.

5.1. Bilinear inelastic SDOF system

The material possesses an initial stiffness k_1 during the linear stage. Subsequently, the material behaves nonlinearly with a degrading stiffness k_2 (less than k_1) under large

amplitudes. The parameter $\gamma = \frac{k_2}{k_1}$ is known as the strain-hardening ratio (see figure 3). The strain-hardening ratio ranges from zero for elastic-plastic behavior to a fracture less than 1. Note that $\gamma = 1$ implies linear behavior. The response of elastic-plastic structures represents a special case of the bilinear structures (k_2 = 0).

The nonlinear equation of motion governing the response of a SDOF system is given as:

$$m\ddot{u}(t) + c\dot{u}(t) + f_s(t) = f(t) \tag{17}$$

Where m, c are the mass and damping of the SDOF system, $u(t)$ is the displacement response, $\dot{u}(t)$ is the velocity response, ü(t) is the acceleration response, $f_s(t)$ is the nonlinear restoring force in the spring and $f(t)$ is the blast force to the SDOF system. The above equation of motion may describe the dynamic response of a single-story building structure under a blast load. As discussed earlier, for linear structural behavior the restoring force $f_s(t)$ is a linear function of the displacement response $u(t)$ and the spring stiffness coefficient k_1. Whereas, in the more general case, when structural nonlinearities are considered, $f_s(t)$ is a nonlinear function of the structure response. Thus, the restoring force is a function of the displacement response and the velocity response.

For nonlinear dynamical systems with elastic-plastic characteristics ($k_2 = 0$), the above equation of motion may be re-written as:

$$\ddot{u}(t) + 2\varsigma\omega\dot{u}(t) + \omega^2 u_y \bar{f}_s(u, \dot{u}) = \frac{f(t)}{m} \tag{18}$$

Where $\varsigma = c/2\sqrt{k_1 m}$ is the damping ratio and u_y is the yield displacement. It may be recalled that, at larger amplitudes the natural vibration period is not defined for bilinear systems. The function $\bar{f}_s(u, \dot{u})$ may be defined as the spring restoring force in a dimensionless form.

Referring to the above equation, it may be noted that for a given blast load $f(t)$, the displacement response depends on the natural frequency ω, the damping ratio ς and the yield displacement u_y as shown in figure 3-a. Herein, the yield displacement u_y is defined as f_y/k_1 where f_y is the yield stress. The dynamic analysis of bilinear structures governed by the above equation of motion can be carried out directly by solving this equation. Alternatively, the dynamic analysis of these systems can be characterized in terms of the bilinear displacement response normalized to the yield displacement. This dimensionless quantity is known as the ductility factor. Thus, defining this factor as $\mu(t) = u(t)/u_y$ and substituting into Equation. (18), one obtains

$$\ddot{\mu}(t) + 2\varsigma\omega\dot{\mu}(t) + \omega^2 u_y \bar{f}_s(\mu, \dot{\mu}) = \frac{f(t)}{u_y m} \tag{19}$$

It follows from this equation of motion that the ductility factor for systems driven by a time-variant dynamical load is also a time-variant quantity. It may be observed that the expressions $\ddot{u}(t) = u_y\, \ddot{\mu}(t)$ and $\dot{u}(t) = u_y\, \dot{\mu}(t)$ were employed in deriving the above equation. The constant $a_y = F_y/m$, appearing on the right side of this equation, can be interpreted as the acceleration of the mass necessary to produce the yield force F_y and $\bar{f}_s(\mu, \dot{\mu})$ is the force–deformation relation in dimensionless form. The response analysis of bilinear systems governed by the above equation of motion is generally carried out using step by step numerical integration techniques.

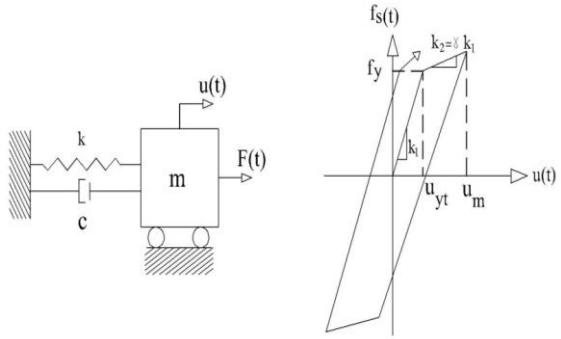

(a) (b)

Fig. 3. (a) SDOF system **(b)** Bilinear force-displacement relation.

6. Dissipated energy under blast loads

Moustafa [42] and [43] provided an overview on the dissipated energy for SDOF structures under earthquake loads. These energy terms can be quantified by integrating the structure equation of motion [43, 44, 45, 46 and 47]. These energy quantities could be estimated based on the absolute or the relative response of the structure. There are some differences between relative energy equation and absolute energy equation [46]. In this paper, the relative equation is used. The energy balance for the bilinear system can be written as:

$$\int_0^u m\ddot{u}(t)\,du + \int_0^u c\dot{u}(t)\,du + \int_0^u f_s\,du = \int_0^u f(t)\,du \tag{20}$$

Equation (21) presents the energy balance equation, which can be written as:

$$E_{\mathrm{kr}}(t) + E_{\mathrm{d}}(t) + E_{\mathrm{a}}(t) = E_{\mathrm{ir}}(t) \tag{21}$$

where E_{kr} is the relative kinetic energy ($E_{\mathrm{kr}} = \frac{1}{2}m\dot{u}^2$). It should be noted that E_{d} is the energy absorbed by damping. It can be shown that [48]:

$$E_{\mathrm{d}}(\mathrm{t}) = \int_0^t c\dot{u}^2\,dt = \int_0^t c\frac{2E_{\mathrm{kr}}}{m}\,dt = 4\omega\varsigma\int_0^t E_{\mathrm{kr}}\,dt \tag{22}$$

On the other hand, the absorbed energy E_{a}, which consists of the recoverable elastic strain energy E_{s} and hysteretic energy E_{h}. The absorbed energy is obtained as:

$$E_{\mathrm{a}}(t) = \int_0^u f_s(u,\dot{u})du = E_{\mathrm{s}} + E_{\mathrm{h}} \tag{23}$$

$$E_{\mathrm{s}}(t) = \frac{{f_{\mathrm{s}}}^2}{2k_1} \tag{24}$$

$$E_{\mathrm{H}}(t) = E_{\mathrm{a}}(t) - E_{\mathrm{s}}(t) \tag{25}$$

Where k_1 is the initial stiffness of the SDOF bilinear structure.

E_{ir} is the relative input energy . It may be written as:

$$E_{\mathrm{ir}}(t) = \int_0^u f(t)\,du = \int_0^t f(t)\dot{u}(t)dt \tag{26}$$

The next section explains the use of the response parameters and plastic energy in developing damage indices.

7. Damage size of inelastic structures under blast loads

Previous research work has quantified damage of structures in terms of damage indices [43, 49 and 50]. There are many researches that discussed define of the structural damage such as: (1) Yao and Yeh [51] defined structural damage as deficiency and deterioration of any structural characteristic caused by external loads. This damage could occur to a structural member or to the connection of two structural members in the form of cracks or rotation, (2) Chung *et al*. [52] defined damage as the degradation of a member with certain consequences regarding the member's capacity to resist further load, (3) FEMA 306 [53] defined damage as the physical evidence of bilinear deformation of a structural member and (4) Hwang and Scribner [54] defined collapse as a damage state that the member strength at maximum deformation has dropped below seventy–five percent of its initial yield strength. Likewise, Park and Ang and Pauley and Priestley [55 and 56] considered a twenty percent drop in strength as the failure criterion for reinforced concrete members. It is generally accepted that damage in structural members can be due to excessive ductility demand and cumulative hysteretic action [55, 57, 58, 59, 60, 61and 62].

Ductility is the best–known and probably the most widely used index in damage assessment [63, 64 and 65]. Recent studies have shown that ductility is not a reliable damage index by itself since it does not account for the influences of the duration of the frequency content, strong shaking and the cumulative bilinear deformation [47, 61, 66, 67 and 68]. Powell and Allahabadi [69] proposed a damage index in terms of the ultimate ductility μ_u and the maximum ductility μ_{max}:

$$DI_{\mu} = \frac{u_{\mathrm{m}} - u_{\mathrm{y}}}{u_{\mathrm{u}} - u_{\mathrm{y}}} = \frac{\mu_{\mathrm{max}} - 1}{\mu_{\mathrm{u}} - 1} \tag{27}$$

However, DI_{μ} does not include effects from hysteretic energy dissipation.

Cosenza et al [49] and Fajfar [67] proposed a damage index based on the structure hysteretic energy E_{H} and:

$$DI_{\mathrm{H}} = \frac{E_{\mathrm{H}}/(F_{\mathrm{y}} u_{\mathrm{y}})}{\mu_{\mathrm{u}} - 1} \tag{28}$$

A robust damage measure should include not only the maximum response but the effect of repeated cyclic loading as well. Park and coworkers developed a simple damage index [55, 70 and 71]:

$$DI_{\mathrm{PA}} = \frac{u_{\mathrm{max}}}{u_{\mathrm{u}}} + \beta \frac{E_{\mathrm{H}}}{F_{\mathrm{y}} u_{\mathrm{u}}} = \frac{\mu_{\mathrm{max}}}{\mu_{\mathrm{u}}} + \beta \frac{E_{\mathrm{H}}}{F_{\mathrm{y}} u_{\mathrm{y}} \mu_{\mathrm{u}}} \tag{29}$$

where, u_{max} is the maximum absolute value of the displacement, u_{u} is the ultimate deformation, u_{y} is the yield displacement, E_{H} is the dissipated hysteretic energy, β is a positive constant that weighs the effect of cyclic loading on structural damage, to assess the structure safety, Eq. (29) was used to estimate the damage index of the structure subjected to the blast load. On the basis of the recommendation of Park *et al.*, the factor β for steel structures is equal 0.025 [71] and [72]. Note that, the variation of the value β is considered in this study.

DI_{PA} is the Park and Ang damage index and $\mathrm{F_y}$ is the yield force. The state of the structural damage is defined as: (a) repairable damage, when $DI_{\mathrm{PA}} < 0.40$, (b) damaged beyond repair, when $0.40 \leq DI_{\mathrm{PA}} < 1.0$, and (c) total or complete collapse, when $DI_{\mathrm{PA}} \geq 1.0$ [70].

A scalar index representing the accumulated damage can be obtained by estimating the area under the Park and Ang damage index as follows:

$$I_{\mathrm{PA}} = \int_0^{t_f} DI_{PA}(\tau)d\tau \tag{30}$$

Referring to Eq. (30), an energy index representing the normalized cumulative hysteretic energy developed by Fajfar [49] and Cosenza [67] can be obtained as follows:

$$I_{\mathrm{CF}} = \frac{1}{f_y\, u_y(\mu_u - 1)} \int_0^{t_f} E_H(\tau)d\tau \tag{31}$$

Where $\frac{1}{f_y\, u_y}$ is a constant.

To the best of our knowledge, all the above studies derived mathematical expressions for damage of structures to earthquakes. In this study, we employ some of these expressions in estimating damage of structures to blast loads.

8. Numerical results and discussion

To illustrate the formulation developed in this study, the dynamic response of a simple structure, modeled as a damped bilinear SDOF system under blast load, is presented in this section. The static overpressure, the response displacement, the dissipated hysteretic kinetic, damping and input energies and damage indices are evaluated. The total mass of the structure is taken as 2×10^3 kg and the initial stiffness = 2×10^5 N/m. The yield displacement in tension and compression is taken as 0.01 and -0.01 m, respectively. The parameters of the blast load are taken as the charge weight w = 2000 kg of TNT, the scaled distance z = 0.40 and the stand-off distance R = 5 m. Herein, $p_{\mathrm{smax}} = 1.10 \times 10^2$ kN/m^2, maximum blast force $f_{max} = f(0) = 1.95 \times 10^2$ kN and the time duration of the positive and negative pressures are $t_{\mathrm{d}^+} = 0.018$ s and the total duration, $t_{\mathrm{d}} = 0.05$ s, respectively.

The numerical results of the parametric study carried out in this section for the response of SDOF structure under blast load are illustrated in figures 5 to 9 and demonstrated in tables 2 to 8. Based on an extensive investigation of the numerical results obtained, the following remarks are drawn:

1- The structure oscillates a way from its equilibrium position and system returns back to rest by the end of the duration explosion load keeping a permanent deformation. The amplitude of the displacement response starts to build up until it reaches its maximum value u_{m} of 0.19 m at about 0.09 s and subsequently it starts to decay keeping permanent deformation of 0.01 m at about 1 s. Unlike, the elastic system, the bilinear structure after yielding does not oscillate about its initial equilibrium position. Yielding causes the structure to drift from its initial equilibrium position and system oscillates around a new equilibrium position until this gets shifted by another yielding. Accordingly, after the explosion ends the structure comes to rest at a position different from its initial equilibrium position. For instant, when $\varsigma = 0.01$ and $\gamma = 0.20$, the permanent deformation $u_{\mathrm{p}} = 0.01$ m, the maximum absolute ductility ratio $\mu_u = 6.39$, the maximum yielding energy $\mathrm{E_{H_{max}}} = 1.37$ kN m and the maximum damping

energy $E_{d_{max}} = 0.13$ kN m, $DI_{PA} = 1.28$ (damaged beyond repair) and additionally, $I_{PA} = 7.68$ and $I_{CF} = 4.86$ (see figure 4 and tables 4 and 5).

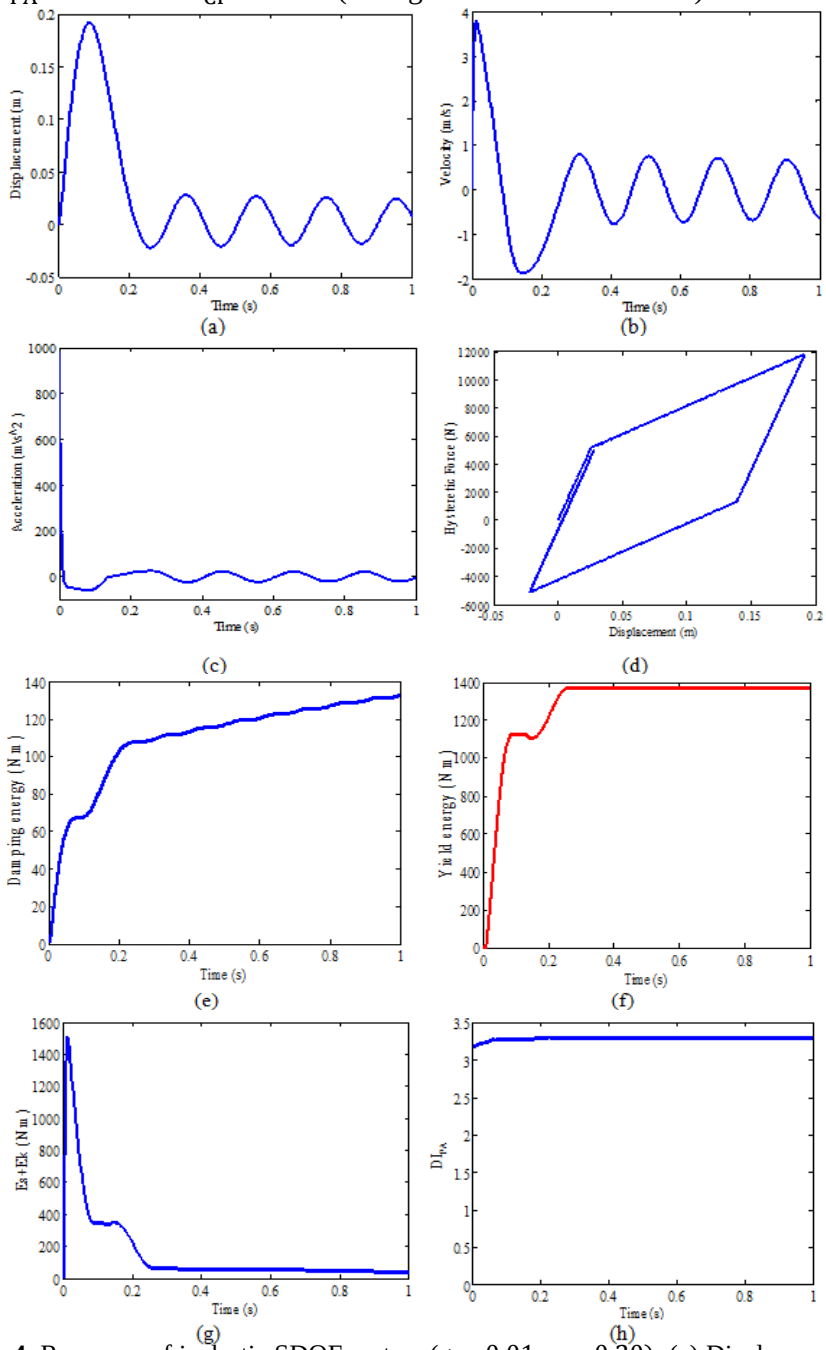

Fig. 4. Response of inelastic SDOF system ($\varsigma = 0.01, \gamma = 0.20$), (a) Displacement response, (b) Velocity response, (c) Acceleration response, (d) Hysteretic loop, (e) Damping energy, (f) Yield energy, (g) Strain and Kinetic energy, (h) Park and Ang damage index.

2- The structural response to the blast load depends on the charge weight and the stand-off distance. For the same charge weight the increase in the stand-off distance is associated with a decrease in the response and dissipated energies of the structure.

The state of the structure damage is changed from total collapse to repairable damage (see table 2). The increase of the stand-off distance with constant ς = 0.01, $\gamma = 0.10$ is associated with a decrease in cumulative damage indices and cumulative yield energy (see Table 3). For instant, when the scaled distance z increases from 0.30 to 0.80 and constant ς = 0.01, $\gamma = 0.10$, u_{m} decreases from 0.48 m to 0.02 m (96%), u_{p} decreases from 0.23 m to 0.005 m (98%), $\mathrm{E}_{\mathrm{d}_{\max}}$ decreases from 0.47 to 0.03 kN m (94%) and $\mathrm{E}_{\mathrm{H}_{\max}}$ decreases from 4.28 to 0.05 kN m (99%). DI_{PA} decreases from 3.73 to 0.15 (96%). The state of the structure damage is changed from total collapse to repairable damage. Indeed, I_{PA} decreases from 22.36 to 0.9 (96%) and I_{CF} decreases from 28.39 to 0.05 (99.8%).

Table 2.
Effect of scaled distance on response of bilinear SDOF (ς = 0.01, = 0.10).

z	u_{m} (m)	u_{p} (m)	μ_u	$\mathrm{E}_{\mathrm{H}_{\max}}$ (kN m)	$\mathrm{E}_{\mathrm{d}_{\max}}$ (kN m)	DI_{PA}	Damage status
0.30	0.48	0.23	17.80	4.28	0.47	3.73	Total collapse
0.40	0.22	0.11	1.60	1.42	0.10	0.28	Repairable damage
0.80	0.02	0.005	1.20	0.05	0.03	0.15	Repairable damage

Table 3.
Effect of scaled distance on cumulative damage indices and cumulative energy (ς = 0.01, $\gamma = 0.10$).

z	I_{PA}	I_{CF}
0.30	22.36	28.39
0.40	1.68	5.10
0.80	0.90	0.05

3- The total duration t_{d} of the blast load is seen to affect the structural response. As the total duration increase, the yield energy increases and larger number of stress reversals are observed. For example, for $\varsigma = 0.02$ and γ = 0.20 maximum displacement, permanent deformation, maximum hysteretic energy, damping energy and Park and Ang damage index are 0.18 m, 0.02 m, 1.28 kN m, 0.24 kN m and 0.93 to $t_{\mathrm{d}} = 0.05$ s. These values become 0.26 m, 0.12 m, 1.68 kN m, 0.26 kN m and 1.92 for $t_{\mathrm{d}} = 0.04$ s. On the other hand, the increase of the total duration with constant $\varsigma = 0.02$ and γ = 0.20 is associated with increase in cumulative damage indices and cumulative yield energy (I_{PA} increases from 4.58 to 12.20 and I_{CF} increases from 5.58 to 6) as shown in figure 4.

4- The influence of a decrease in the damping ratio ς with constant γ = 0.20 is seen to be associated with an increase in the maximum displacement and the yielding energy. On the other hand, the permanent deformation and the damping energy are decreased (see figure 5 and table 4). For instant, when damping ratio decreases from 0.03 to 0.01 and constant $\gamma = 0.20$, u_{m} increases from 0.17 m to 0.19 m (12%), u_{p} decreases from 0.03 m to 0.01 m (67%), $\mathrm{E}_{\mathrm{d}_{\max}}$ decreases from 0.32 to 0.13 kN m (59%) and $\mathrm{E}_{\mathrm{H}_{\max}}$ increases from 1.21 to 1.37 kN m (13%). The state of the structure damage is changed from damaged beyond repair to total collapse. The increase in damping ratio with constant γ = 0.20 is associated with decrease in cumulative damage indices and cumulative yield energy (see table 5).

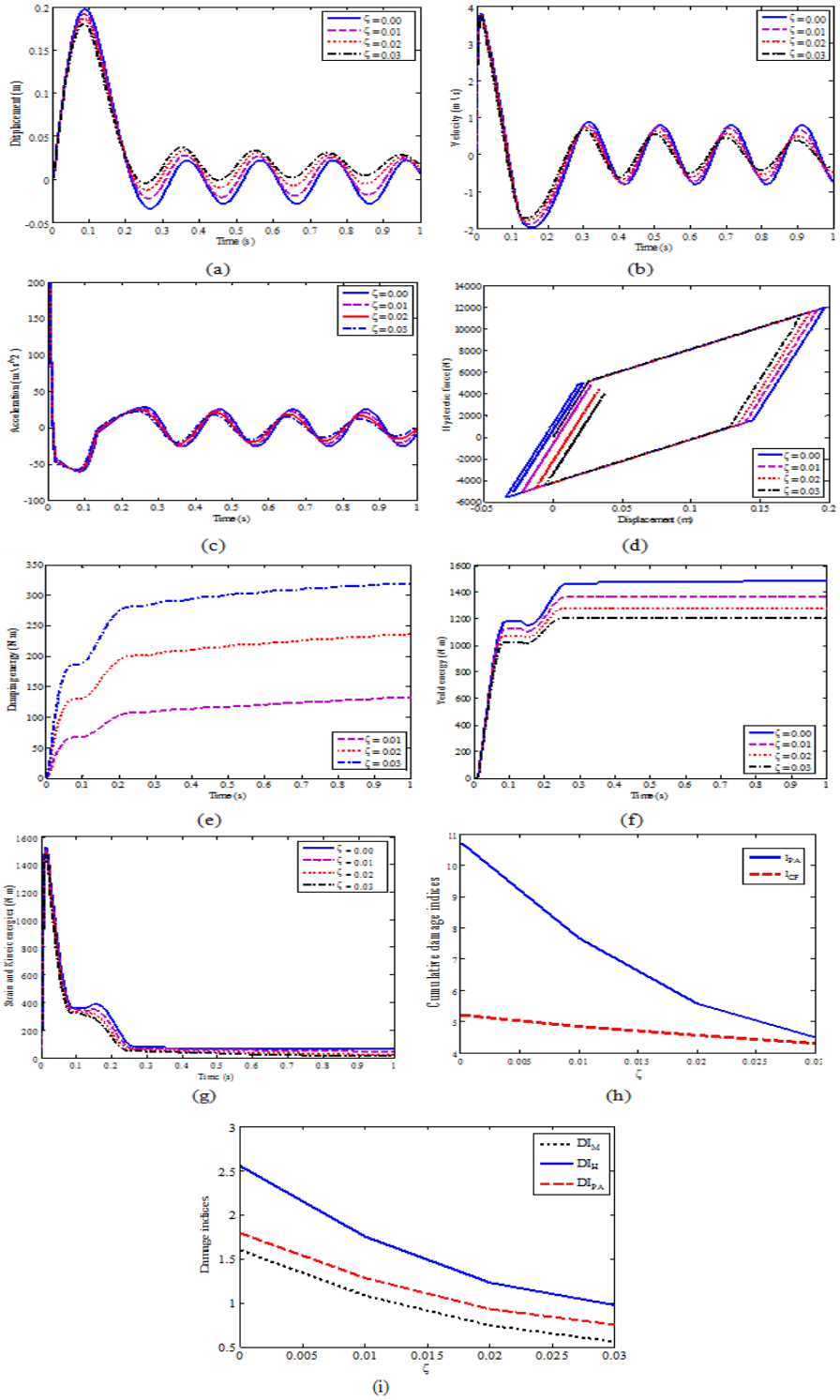

Fig. 5. Effect of damage ratio on response of inelastic SDOF system ($\gamma = 0.20$) (a) Displacement response, (b)Velocity response, (c) Acceleration response, (d) Hysteretic loop, (e) Damping energy, (e)Yield energy, (e) Strain and Kinetic energies, (h) Cumulative damage indices, (i) Ductility damage index , Cosenza and Fajfar damage index and Park and Ang damage index.

Table 4.
Effect of damping ratio on structure response (γ = 0.20).

ς	u_{m} (m)	u_{p} (m)	μ_u	$\mathrm{E}_{\mathrm{H_{max}}}$ (kN m)	$\mathrm{E}_{\mathrm{d_{max}}}$ (kN m)	DI_{PA}	Damage status
0	0.20	0.01	8.85	1.48	0	1.79	Total collapse
0.01	0.19	0.01	6.39	1.37	0.13	1.28	Total collapse
0.02	0.18	0.02	4.67	1.28	0.24	0.93	Damaged beyond repair
0.03	0.17	0.03	3.79	1.21	0.32	0.75	Damaged beyond repair

Table 5*.*
Effect of damping ratio on cumulative damage indices (γ = 0.20).

ς	I_{PA}	I_{CF}
0	10.73	5.22
0.01	7.68	4.86
0.02	5.58	4.58
0.03	4.50	4.32

5- The increase in the strain-hardening ratio γ with constant $\varsigma = 0.02$ is seen to be associated with a decrease in the maximum displacement, permanent deformation and yield energy. On the other hand, the damping energy is increased (see figure 6 and table 6). For instant, when the strain-hardening ratio increases from 0.05 to 0.20 and constant with $\varsigma = 0.02$, u_{m} decreases from 0.24 m to 0.19 m (21%) while u_{p} decreases from 0.17 m to 0.02 (88%). At the same time $\mathrm{E}_{\mathrm{H_{max}}}$ decreases from 1.33 to 1.28 kN m (3.8%) and $\mathrm{E}_{\mathrm{d_{max}}}$ decreases from 0.20 to 0.18 kN m (10%). The state of the structure damage is changed from repairable damage to damage beyond repair. The increase in strain-hardening ratio with constant $\varsigma = 0.02$ is associated with increase in cumulative damage indices related to the increase in DI_{PA} (Because there is a direct relationship between them). Also, the increase in strain-hardening ratio with constant $\varsigma = 0.02$ is associated with decrease in cumulative yield energy related to the decrease in $\mathrm{E}_{\mathrm{H_{max}}}$ (see tables 6 and 7).

Table 6.
Effect of strain hardening ratio on structure response ($\varsigma = 0.02$).

γ	u_{m} (m)	u_{p} (m)	μ_u	$\mathrm{E}_{\mathrm{H_{max}}}$ (kN m)	$\mathrm{E}_{\mathrm{d_{max}}}$ (kN m)	DI_{PA}	Damage status
0	0.28	0.25	1.00	1.35	0.22	0.19	Repairable damage
0.05	0.24	0.17	1.20	1.33	0.20	0.22	Repairable damage
0.10	0.22	0.11	1.50	1.31	0.19	0.30	Repairable damage
0.20	0.19	0.02	4.67	1.28	0.18	0.93	Damaged beyond repair

Table 7*.*
Effect of strain hardening ratio on cumulative damage indices ($\varsigma = 0.02$).

γ	I_{PA}	I_{CF}
0	1.14	4.80
0.05	1.32	4.79
0.10	1.74	4.66
0.20	5.58	4.58

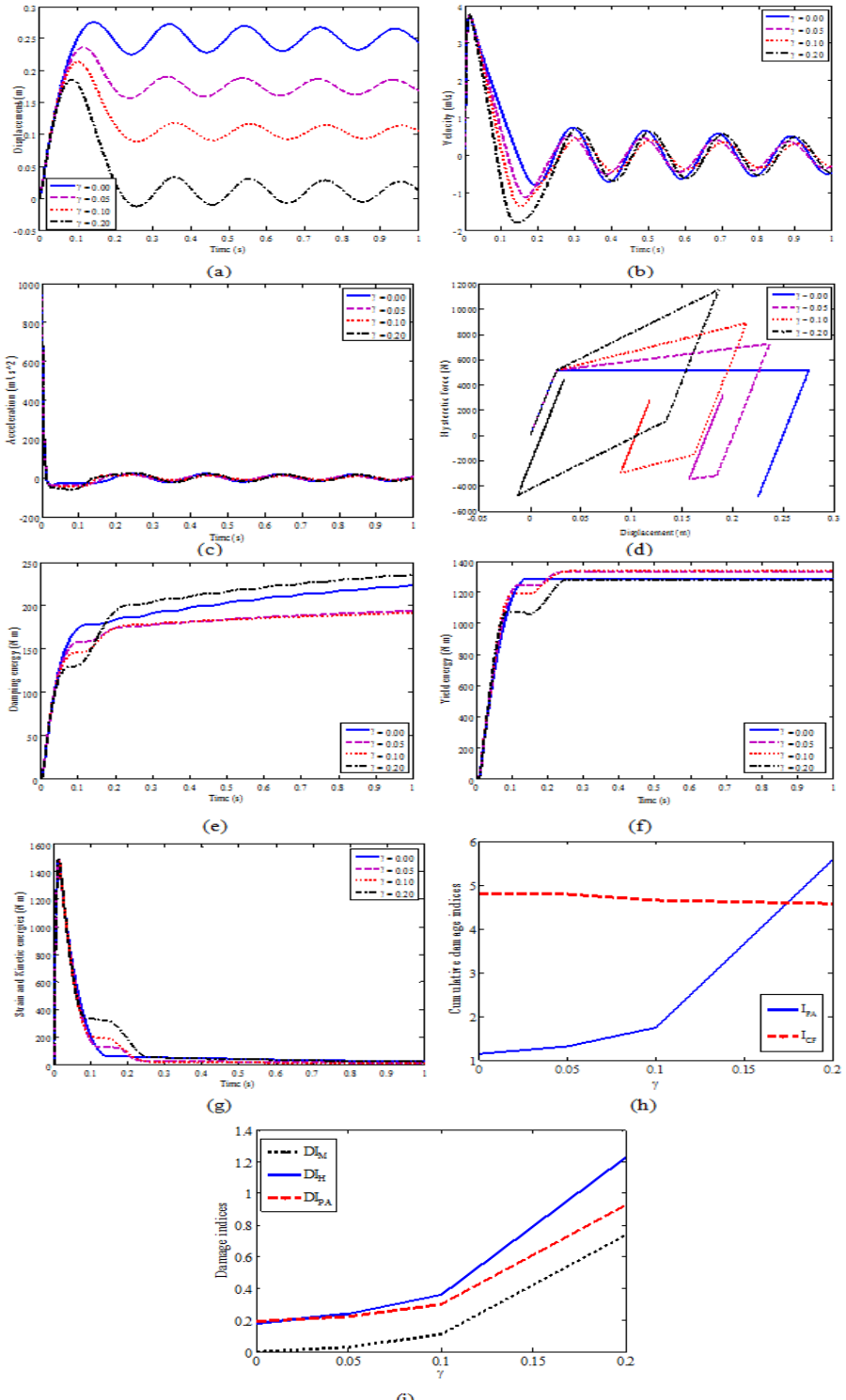

Fig. 6. Effect of strain hardening ratio on response of inelastic SDOF system ($\varsigma = 0.02$) (a) Displacement response, (b)Velocity response, (c) Acceleration response, (d) Hysteretic loop, (e) Damping energy, (e)Yield energy, (e) Strain and Kinetic energies, (h) Cumulative damage indices, (i) Ductility damage index , Cosenza and Fajfar damage index and Park and Ang damage index.

6- The effect of initial natural frequency on response of bilinear SDOF with constant $\varsigma = 0.01$ and $\gamma = 0.10$ is shown in Table 8. The decrease of ω is associated with a decrease in the response, dissipated energies and damage indices of the structure. Thus, for $\omega = 44.70$ rad/s, the damage status is damaged beyond repair, while for $\omega = 25.80$ rad/s, the damage status is repairable damage.

Table 8.
Effect of initial natural frequency on response of bilinear SDOF ($\varsigma = 0.01, = 0.10$).

ω (rad/s)	u_m (m)	u_p (m)	μ_u	$E_{H_{max}}$ (kN m)	$E_{d_{max}}$ (kN m)	DI_{PA}	Damage status
44.70	0.36	0.13	3.50	2.80	0.25	0.60	Damaged beyond repair
31.60	0.22	0.11	1.61	1.42	0.10	0.28	Repairable damage
25.80	0.17	0.07	1.50	0.95	0.08	0.25	Repairable damage

7- Figure 7 shows the influence of changing the value of β on the Park and Ang damage index. It is seen that β is directly proportional to DI_{PA} with a linear relation. For instant, when β increases from 0 to 0.20 with constant $\varsigma = 0.01$ and $\gamma = 0.20$, DI_{PA} increases from 1.08 to 1.35.

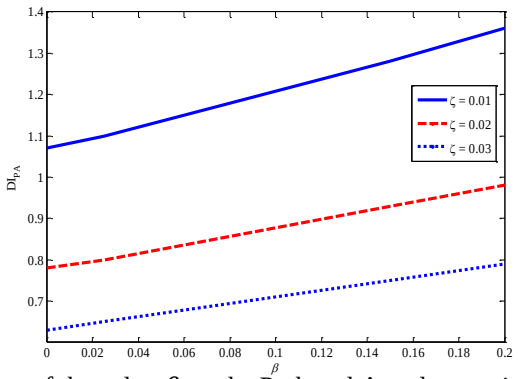

Fig. 7. Effect of the value β on the Park and Ang damage index, $\gamma = 0.20$

8- The influence of the variation of the damping ratio on the structure elastic-plastic deformation ($k_2 = 0$) was seen to be significant. As might be expected, with increasing the damping ratio, the structure maximum elastic-plastic response is seen to be reduced (see figure 8). Thus, the structure maximum elastic-plastic deformation was computed to be 0.29 m for $\varsigma = 0.01$. This value reduces to 0.26 if $\varsigma = 0.03$ (10%). Thus when damping ratio increases from 0.01 to 0.03, u_p decreases from 0.26 m to 0.23 m (11.50%). At the same time $E_{H_{max}}$ decreases from 1.37 to 1.21 kN m (11.70%) and $E_{d_{max}}$ increases from 0.12 to 0.31 kN m (158%).

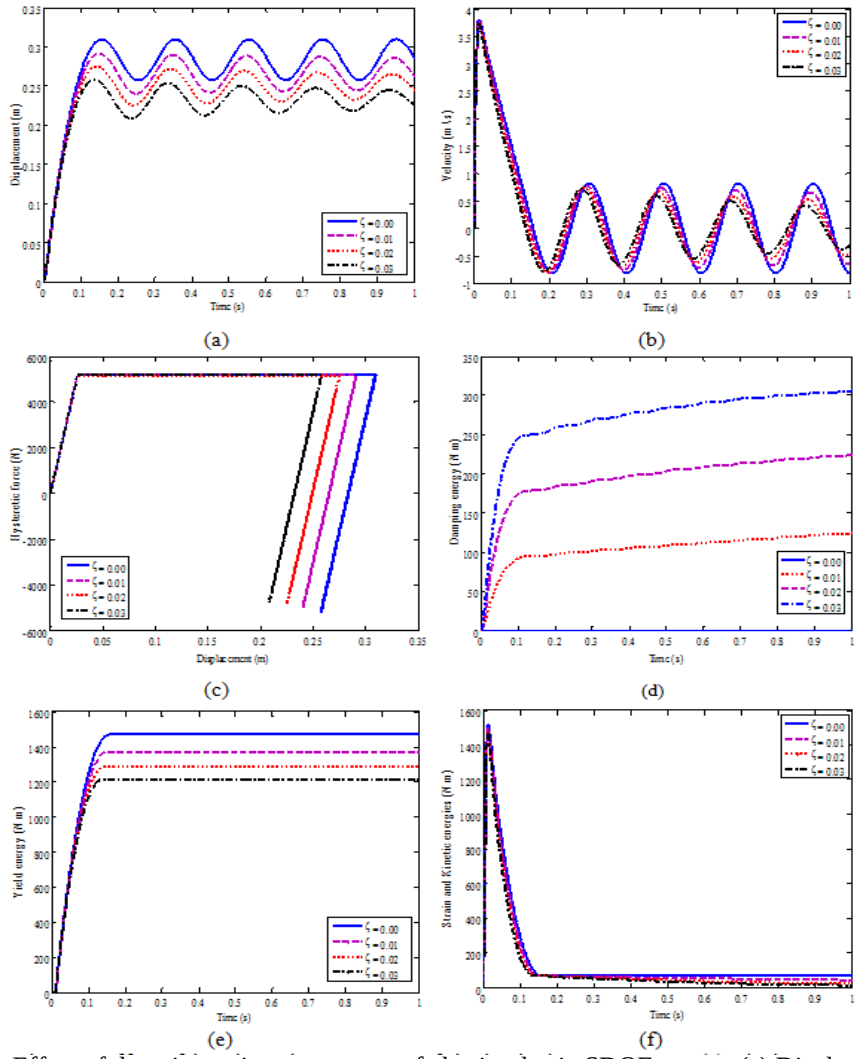

Fig. 8. Effect of damping ratio on response of elastic-plastic SDOF system (a) Displacement response, (b) Velocity response, (c) Hysteretic loop, (d) Damping energy, (e)Yield energy, (f) Strain and Kinetic energies

9. Conclusions, Recommendations and Future work

This section presents the overall conclusions of this research. The performance of high-risk facilities such as public, commercial and industrial structures under extreme loads such as explosions and high velocity impact is an important problem. This study investigated the blast response and damage analysis of simple structures under blast loads. The structure is modeled as SDOF system with bilinear or elastic-plastic force-displacement relation. The blast load is modeled as a time-series of decaying amplitude with positive and negative pressure zones. The blast load is defined in terms of charge weight in TNT, off-set distance and scaled distance. The equation of motion governing the response for inelastic SDOF system is solved using Newmark β method in the MATLAB-platform [1]. The structural response is estimated using maximum and permanent displacement, input, irrecoverable hysteretic, damping, kinetic and recoverable elastic

strain energies. The damage status of the structure is quantified using Park and Ang damage indices. Damage indices make it possible to decide necessary structural repair. The conclusions can be summarized as follows:

(1) The structural response and associated damage level depend on the explosion load characteristics in terms of charge weight and stand-off distance. The damage level increases with increase in charge weight and decrease in stand-off distance.

(2) Damage level depends on material properties such as damping ratio, strain-hardening ratio and yield strength. Damage is seen to be inversely proportional to damping and directly proportional to strain hardening ration.

(3) Input energy to the inelastic structure is dissipated mainly by yielding and damping. The inelastic structure after yielding oscillates around a new equilibrium position and does not return back to its initial equilibrium position developing permanent deformation.

(4) This research could be extended to more complex structures such as skeletal buildings composed of RC walls and slabs and nuclear power plants using the finite element method. The blast load could be modeled within the framework of probabilistic analysis. Herein, the structural response will be a random process characterized in terms of its moments such as mean and standard deviation. Future research could include the development of a new damage index to quantify damage of structures under blast loads. The extension of the work to account for more accurate material behavior models such as tri-linear and fiber model needs to be investigated as a future work. The work could also be extended to account for the simultaneous occurrence of two or more loads such as earthquake and blast loads or blast and fire loads or blast and impact and fire loads using the finite element method.

(5) Guidelines on extreme load and provisions on progressive collapse prevention and improving ductility of structural members should be included in current building regulations and design standards.

REFERENCES

[1] Hill, M., Introduction to Matlab solutions manual, 2013.

[2] Biggs, J. M., Introduction to structural dynamics. Chapter 7: Blast-resistant design. McGraw-Hill, NY, 1964.

[3] Moon, Nitesh N. Prediction of Blast Loading and its Impact on Buildings, Department of Civil Engineering, National Institute of Technology, Rourkela, 2009.

[4] Ngo, T., Mendis, P.; Gupta, A.; Ramsay, J. Blast loading and blast effects on structures – An overview. EJSE Special Issue: Loading on Structures, 2007.

[5] U.S. Department of the Army. 1990.Structures to resist the effects of accident explosions. TM 5-1300, Navy NAVFAC P-397, AFR 88-2. Washington, DC: Departments of the Army, Navy and Airforce.

[6] Alaoui, S and Oswald, C., Blast-resistant design considerations for precast, prestressed concrete structures, PCI journal, 2007.

[7] Smith, S. J., McCaann, D.M., Blast resistant design of reinforced concrete structures, 2007.

[8] Indian Standard Criteria for blast resistant design of structures for explosion above ground, IS: 4991-1968: Bureau of Indian standards, New delta, 38 P.

[9] U.S. Army manual TM 5-855-1, Fundamentals of Protective Design for Conventional Weapons, U.S. Department of the Army, Washington DC, 1987.

[10] American Society for Civil Engineers (ASCE) 7-02., Combination of loads, pp 239-244, 1997.

[11] Eurocode 1, Actions on structures, General actions, Accidental actions, BS EN 1991-1-7, 2006.

[12] U.S. Army Corps of Engineers. Single degree of freedom structural response limits for antiterrorism design. PDC-TR 06-08. Army Corps of Engineers, 2006.
[13] Canadian Standard Association CSA S850, Design and assessment of buildings subjected to blast loads, Canada, 126 P, 2012.
[14] Brode, H.L., Numerical solution of spherical blast waves, Journal of Applied Physics, American Institute of Physics, Ney York, 1955.
[15] Henrych, J. The dynamics of explosion and its use elsevier science Publisher, 1979.
[16] Kingery C. N., and Bulmash G., Airblast parameters from TNT spherical air burst and hemispherical surface burst, Defence Technical Information Centre, Ballistic Research Laboratory, Aberdeen Proving Ground, Maryland, 1984.
[17] Smith P.D., Hetherington J. G., Blast and ballistic loading of structures. Butterworth Heinemann, 1994.
[18] Kinney, G. H., Graham, K. J., Explosive shocks in air, The Macmillan Company, New York, 1962.
[19] Liepmann H.W. and Roshko A. Elements of gas dynamics. John Wiley, New York, 1957.
[20] Longinow A, and Mniszewski KR., Protecting buildings against vehicle bomb attacks, Practice periodical on structural design and construction, ASCE, New York, pp. 51-54, 1996.
[21] Mays G.C., Smith P.D., Blast effects on buildings, Thomas Telford Publications, Heron Quay, London, 1995.
[22] Mays, G. C.; Smith, P. D., Blast effects on buildings – Design of buildings to optimize resistance to blast loading, Tomas Telford, 2001.
[23] Mills, C.A., The design of concrete structure to resist explosions and weapon affects, Proceedings of the 1st Int. Conference on concrete for hazard protections, Edinburgh, UK, pp. 61-73, 1987.
[24] Newmark, N. M. and Hansen, R.J., Design of blast resistant structures, Shock and Vibration Handbook, Vol. 3, Eds. Harris and Crede. McGraw-Hill, New York, USA 1961.
[25] Fertice, D. G., Dynamics and Vibration of Structures, A wiley-interscience publication, pp. 343-434, 1973.
[26] LZA, T. T., Gilsanz M. S., Interim life safety report, 30 West Broadway, New York, NY. Prepared for New York City Department of Design and Construction, 2001.
[27] LZA, T. T., Guy, J., WTC emergency damage assessment of buildings. Structural Engineers Association of New York Inspections of September and October 2001, Draft prepared for the New York City Department of Design and Construction. New York, NY, est. April 2002.
[28] Vrom, B., Effecten van explosive op constructures, Technical report, 2003.
[29] Vrom., B, Methods for the calculation of physical effects due to releases of hazardous materials (liquids and gasses), Technical report, 2005.
[30] Marchand K. A., UFC 4 -023-03 Design Of Buildings to Resist Progressive Collapse, U. G. S. Dept. of Defence and Administration, Washington, 2005.
[31] Bangash, M. Y. H., Bangash, T., Explosion-Resistant Buildings Design, Analysis and Case Studies, Springer, Berlin, 2006.
[32] Baker, W. E., Cox, P.A., Westine, P.S., Kulesz, J.J. and Strehlow, R.A., Explosion hazards and evaluation, Elsevier Scientific Publishing Company, New York, 1983.
[33] Dharaneepathy M.V., Rao M.N.K., and Sathakumar A.R., Critical distance for blast-resistant design, Computer and Structures, Volume 54-4, Pages 587-595, 1995.
[34] Baker W.E., Explosions in Air, Univ. of Texas Press, Austin TX USA, 1973.
[35] Rankine W. J. H., On the thermodynamic theory of waves of finite longitudinal disturbance. Phil. Trans. Roy. Soc., 160, 277-288, 1870.
[36] Gutenberg. b., Richter. c. f., Earthquake magnitude, intensity, energy, and acceleration, 1956.
[37] Von, B., Krehl, P, O, K., History of Shock Waves, Explosions and Impact, 2008.
[38] Chopra, A. K., Dynamics of structures, third ed., Pretence-Hall, Englewood Cliffs, NJ, 2006.
[39] Clough, R.W. and Penzien, J., Dynamics of structures, Chapter 24: Seismological Background, third ed., Computers & Structures Inc., CA, 2003.

[40] Paz, M., and Leigh, W. Structural dynamics, 2010.
[41] Ngo, T., Lam, N.; Mendis, P. Response spectrum solution for blast loading. EJSE international, 2004.
[42] Moustafa, A., Critical seismic load inputs for simple inelastic structures. J. Sound Vib., 296, 949–967, 2006.
[43] Moustafa, A., Damage-Based Design Earthquake Loads for Single-Degree-Of-Freedom Inelastic Structure J. Sound Vol.137, No. 3, 456–46, 2011.
[44] Akiyama, H., Earthquake-resistant limit-state design for buildings. University of Tokyo Press, Tokyo, 1985.
[45] Takewaki, I., Bound of earthquake input energy. Journal of Structural Engineering. 130(9): 1289–1297, 2004.
[46] Uang, C. M., Bertero, V. V., Evaluation of seismic energy in structures. Earthquake Eng. Struct. Dyn., 19, 77–90, 1990.
[47] Zahrah, T. F., and Hall,W. J. Earthquake energy absorption in SDOF structures. J. Struct. Eng., 110, 1757–1772, 1984.
[48] Bruneau, M. and Wang, N. (1996). Some aspects of energy methods for the inelastic seismic response of ductile SDOF structures. Engineering Structures 18:1, 1-12.
[49] Cosenza, C., Manfredi, G., and Ramasco, R. 1993. The use of damage functionals in earthquake engineering: a comparison between different methods. Earthquake Eng. Struct. Dyn., pp. 22, 855–868, 1993.
[50] Ghobara, A., Abou-Elfath, H., and Biddah, A. (1999). Response based damage assessment of structures. Earthquake Engineering Structure Dynamic. 28(1):79–104.
[51] Yao, J.T.P., and Yeh, H.Y., Formulation of Structural Stability, Journal of Structural Engineering, ASCE, December, 1985.
[52] Chung, Y.S., Meyer, C., and Shinozuka, M., A new damage model for reinforced concrete structures, Proceedings of the 9th World Conference on Earthquake Engineering, Tokyo–Kyoto, Japan, Vol. VII, pp. 205-210, 1988.
[53] FEMA 306, Evaluation of earthquake-damaged concrete and masonry wall buildings, Basic Procedures Manual, Federal Emergency Manage Agency, prepared by Applied Technology Council, Washington, D.C., 270 pp, 1999.
[54] Hwang, T.H., and Scribner, C.F., R/C member cyclic response during various loadings, Journal of Structural Engineering, ASCE, Vol. 110, 3, pp. 477-489, 1984.
[55] Park, Y. J., and Ang, A. H.-S. Mechanistic seismic damage model for reinforced concrete. J. Struct. Eng., 111 (4), 722–739, 1985.
[56] Paulay, T., Priestley, M. J. N., Seismic design of reinforced concrete and masonry buildings. Wiley Interscience, New York, N.Y. 28, 1992.
[57] Banon, H., Biggs, J.M., and Irvine, H.M., Seismic Damage in Reinforced Concrete Frames, Journal of Structural Division, ASCE 107, ST9, pp. 1713-1729, 1981.
[58] Elenas, A., and Meskouris, K., Correlation study between seismic acceleration parameters and damage indices of structures, Engineering Structures, Vol. 23, No. 6, pp. 698-704, 2001.
[59] Kasiraj, I., and Yao, J.T.P., Fatigue damage in seismic structures, Journal of Structural Engineering, ASCE, Vol. 95, No. 8, pp. 1673-1692, 1969.
[60] Kunnath, S.K., Reinhorn, A.M., and Park, Y.J., Analytical modeling of inelastic seismic response of R/C structure, Journal of Structural Engineering, ASCE Vol. 116, pp. 996-1017, 1990.
[61] Mahin, S.A., and Bertero, V.V., An evaluation of inelastic seismic design spectra, Journal of Structural Division, ASCE, Vol. 107, No. ST9, pp. 1777-1795, 1981.
[62] Stephens, J.E., and Yao, J.T.P., Damage assessments using response measurements, Journal of Structural Engineering, ASCE, Vol. 113, No. 4, pp. 787 801, 1987.
[63] Carr, A.J., and Tabuchi, M., The structural ductility and the damage Index for reinforced concrete structure under seismic excitations, Proceedings of 2nd European conference on structural dynamics, pp. 169-176, 1993.

[64] Sordo, E., Terán, A., Guerrero, J.J., Juárez, H., and Iglesias, J., The Mexico Earthquake of September 19, 1985—Ductility and Resistance Requirements Imposed on a Concrete Building, Earthquake Spectra, Vol. 5, Issue 1, pp. 41-50, 1989.

[65] Torres, M.A., and Ruiz, S.E., Design Algorithm Based on Probabilistic Seismic Demands for Buildings Rehabilitated with Hysteretic Energy-Dissipating Devices, Earthquake Spectra, Vol. 20, Issue 2, pp. 503-521, 2004.

[66] Basu, B., Gupta, V.K., A note on damage–based inelastic spectra, Earthquake engineering and structural dynamics, Vol.25, pp. 421-433, 1996.

[67] Fajfar, P., Equivalent ductility factors, taking into account low cyclic fatigue. Earthquake Eng. Struct. Dyn., 21, 837–848, 1992.

[68] Kobori, T., Minai, R., Suzuki, Y., On the seismic safety of elasto-plastic structures considering fatigue damage, Proceedings of the 21st Japan National Congress for Applied Mechanics, Theoretical and Applied Mechanics, Vol. 21, pp. 309-321, 1973.

[69] Powell, G. H., and Allahabadi, R. Seismic damage predictions by deterministic methods: concepts and procedures. Earthquake Eng. Struct. Dyn., 16, 719–734, 1988.

[70] Park, Y. J., Ang, A. H.-S., and Wen, Y. K., Seismic damage analysis of reinforced concrete buildings. J. Struct. Eng., 111(4), 740–757, 1985.

[71]Park, Y. J., Ang, A. H.-S., and Wen, Y. K., Damage-limiting aseismic design of buildings. Earthquake Spectra, 3(1), 1–26, 1987.

[72] Ghosh, S., Datta, D., Katakdhond. A. A., Estimation of the Park-Ang damage index for planar multi-story frames using equivalent single-degree systems. J. Struct 33, 2509-2524, 2011.

الطاقة المشتتة والتلفيات للمنشآت غير المرنة تحت تأثير أحمال الإنفجارات

الملخص العربى

إن المنشآت الهامة والحيوية يجب أن يتم تصميمها بحيث تقاوم الأحمال القصوى العابرة كأحمال الصدمات عالية السرعة والإنفجارات. وتصميم المنشآت لمقاومة الإنفجارات يتضمن إحتياطات معمارية وكذلك تصميم العناصر الإنشائية لمقاومة قوى الإنفجارات. وأحمال الإنفجارات يمكن أن تكون داخلية نتيجة إنفجار أنابيب الغاز أو خارجية نتيجة القنابل الكيميائية أو هجوم بسيارة. في الواقع فإن القنابل الإرهابية والهجوم بالسيارات على المنشآت الهامة أصبح حدث ملحوظ في مصر خلال السنوات القلائل الماضية مما تسبب في فقدان أرواح كثيرة وأدى إلى تلف إنشائي كبير وإنهيار العديد من المنشآت الأثرية والمباني الأمنية. ويتناول هذا البحث عرض الإستجابة والأضرار للمنشآت البسيطة احادية الحرية غير المرنة تحت تأثير أحمال الإنفجارات. يتم نمذجة حمل الإنفجار كدالة متغيرة في الزمن تحتوي علي مرحلتي ضغط موجب وضغط سالب. أولاً يتم نمذجة المعادلات التفاضلية غير الخطية للحركة للهياكل غير المرنة تحت تأثير حمل الإنفجار. وبعدها يتم حل هذه المعادلات. وأخيراً يتم تعريف مختلف مصطلحات الطاقه التي يتم تبديدها ومؤشرات الضرر المرتبطة بها. وتم توضيح الدراسة بحساب الطاقة المشتتة والتلف الإنشائي لنظام احادي الحرية تحت تأثير حمل إنفجار عن طريق التكامل العددي لمعادلة حركة المنشأ بإستخدام برنامج MATLAB. ويقترح في هذه الورقة إنشاء مؤشر رقمي جديد (Park and Ang damage index and Cosenza and Fajfar damage index). وهذه المقاييس مهمة لأنها تعطي مقياس كمي عن مستوى التلف الإنشائي والترميم